Pure Appl. Geophys. 170 (2013), 129–138

DOI 10.1007/s00024-012-0474-8

Pure and Applied Geophysics

A Revised Evaluation of Tsunami Hazards along the Chinese Coast in View of the Tohoku-Oki Earthquake

Huimin Helen Jing,[1,2] Huai Zhang,[2] David A. Yuen,[2,3,4] and Yaolin Shi[2]

Abstract—Japan's 2011 Tohoku-Oki earthquake and the accompanying tsunami have reminded us of the potential tsunami hazards from the Manila and Ryukyu trenches to the South China and East China Seas. Statistics of historical seismic records from nearly the last 4 decades have shown that major earthquakes do not necessarily agree with the local Gutenberg-Richter relationship. The probability of a mega-earthquake may be higher than we have previously estimated. Furthermore, we noted that the percentages of tsunami-associated earthquakes are much higher in major events, and the earthquakes with magnitudes equal to or greater than 8.8 have all triggered tsunamis in the past approximately 100 years. We will emphasize the importance of a thorough study of possible tsunami scenarios for hazard mitigation. We focus on several hypothetical earthquake-induced tsunamis caused by M_w 8.8 events along the Manila and Ryukyu trenches. We carried out numerical simulations based on shallow-water equations (SWE) to predict the tsunami dynamics in the South China and East China Seas. By analyzing the computed results we found that the height of the potential surge in China's coastal area caused by earthquake-induced tsunamis may reach a couple of meters high. Our preliminary results show that tsunamis generated in the Manila and Ryukyu trenches could pose a significant threat to Chinese coastal cities such as Shanghai, Hong Kong and Macao. However, we did not find the highest tsunami wave at Taiwan, partially because it lies right on the extension of an assumed fault line. Furthermore, we put forward a multi-scale model with higher resolution, which enabled us to investigate the edge waves diffracted around Taiwan Island with a closer view.

Key words: Tsunami hazard, Chinese coast, Multi-scale simulation.

1. Introduction

Tsunami earthquakes are defined as shocks with marine origins that generate extensive tsunamis but relatively weak seismic waves. They most likely take place in trench regions with large tectonic movement and young folded crustal belts (Fukao, 1979). The Manila trench bordering the South China Sea and the adjacent Philippine Sea plate is an excellent candidate for such tsunami earthquakes to occur (Hayes and Lewis, 1985; Ku and Hsu, 2009; Megawati *et al.*, 2009; Ozawa *et al.*, 2004; Rangin *et al.*, 1988). During the 2006 USGS tsunami source workshop, three subduction zones, the Manila subduction zone, Ryukyu subduction zone and N. Sulawesi subduction zone, were identified as having high potentials to generate hazardous tsunamis (Liu *et al.*, 2009). Japan's 2011 Tohoku earthquake and tsunami, which should not have come as a surprise to the geophysical community (Stein and Okal, 2011; Geller, 2011; Stein *et al.*, 2011), further remind us to revise previous analyses and be aware of the potential tsunami threat from the Manila and Ryukyu trenches to the south and east China coast.

The Gutenberg-Richter relationship (Gutenberg and Richter, 1944) expresses the relationship between the magnitude and total number of earthquakes in a given region and time period of at least that magnitude (Turcotte *et al.*, 2007). $\log_{10} N = a - bM$, where N is the number of events having a magnitude greater than M, and a, b are constants related to the region, respectively. With sufficient long-period earthquake records, we can estimate where or when a potential major earthquake in a specific geographic region could occur. Previous investigations based on the G-R relationship have suggested that the possibility of potential earthquakes

[1] College of Mechanical Engineering and Mechanics, Ningbo University, Ningbo 315211, China. E-mail: huiminjing@gmail.com
[2] Key Laboratory of Computational Geodynamics, Chinese Academy of Sciences, Beijing 100049, Peoples Republic of China.
[3] Department of Earth Sciences, Minnesota Supercomputing Institute, University of Minnesota, Minneapolis, MN 55455-0219, USA.
[4] Minnesota Supercomputing Institute, University of Minnesota, Minneapolis, MN 55455, USA.

with a magnitude of M_w 8.0 or higher in the Manila trench, which may pose a significant threat to South China Sea coastlines, is very low (Liu *et al*., 2007, 2009). However, we found that without sufficient long-term records, the extrapolated possibility of a major earthquake from the G-R relationship is lower than the realistic cases. This means that a potential huge earthquake in the Manila and Ryukyu trenches might be larger than what we have thought before. Moreover, the coastal elevation along the South China Sea is generally low, making it extremely vulnerable to incoming waves with a height of a couple of meters. In particular, many economically important coastal cities, such as Shanghai and Hong Kong, are located in this particular area. They would suffer a devastating disaster because of their low-lying coastlines. Therefore, the importance of a thorough study on possible worst case tsunami scenarios should be emphasized in view of the recent Tohoku-Oki earthquake. Based on our previous work, we will revise the probabilistic evaluation of tsunami hazards generated from larger earthquakes in the Manila and Ryukyu trenches to the southern and eastern part of China.

2. Potential Tsunami Source and Numerical Modeling

2.1. Potential Tsunami Source

With the statistics of historical seismic records from nearly the last 4 decades, we found that major earthquakes do not necessarily agree with the local Gutenberg-Richter relationship. Based on the G-R relationship, we investigated the possibility of a major earthquake in three regions where a devastating tsunami has occurred in the past few years. These three regions are the Japan trench, Sumatran fault and Peru-Chile trench, corresponding to the Tohoku M9.0 earthquake on 11 March 2011, the Sumatra M9.1 earthquake on 26 December 2004 (Catherine *et al*., 2005; Gahalaut *et al*., 2006) and the Chile M8.8 earthquake on 27 February 2010 (Liu *et al*., 2010), respectively. With the historical records from the Network Earthquake International Center catalogs (NEIC) (Sipkin *et al*., 2000), we chose the earthquake events with magnitudes larger than M_w 5.0 and epicenter depths no deeper than 70 km, which are most likely to trigger tsunamis. The selected earthquakes are listed in Table 1.

Using the mathematical expressions describing the G-R relationship, we can calculate the return period of an earthquake with a given magnitude M. $P_M = \frac{T}{N_M}$, where P_M is the return period, T is the time period of the seismic record, and N_M is the number of earthquakes with magnitudes greater than or equal to M, respectively. Considering a strong earthquake and a series of aftershocks will alter the fitted line of the G-R relationship, we calculated the return periods in two cases, before and after the major earthquake (cases B and A). Figure 1 shows the fitted lines of the G-R relationship for the two cases. Figure 1a shows the fitted lines of B cases. In Fig. 1a the time periods of the seismic records for the three regions are from 1 January 1973 to the day just before

Table 1

Earthquake events used to survey the G-R relationship in the Japan trench, Sumatran fault, Peru–Chile trench, Manila trench and Ryukyu trench

Region	Latitude and longitude	Time to (from 1 January 1973)	Total number of the earthquakes
Japan trench	31°N–45°N	2 April 2011	3,433
	137°E–151°E	10 March 2011	2,984
Sumatran fault	7°S–15°N	2 April 2011	2,321
	90°E–104°E	25 December 2004	923
Peru–Chile trench	24°S–48°S	2 April 2011	1,294
	69°W–77°W	26 February 2010	889
Manila trench	4°N–25°N	2 April 2011	2,781
	107°E–125°E		
Ryukyu trench	23°N–33°N	2 April 2011	1,093
	120°E–133°E		

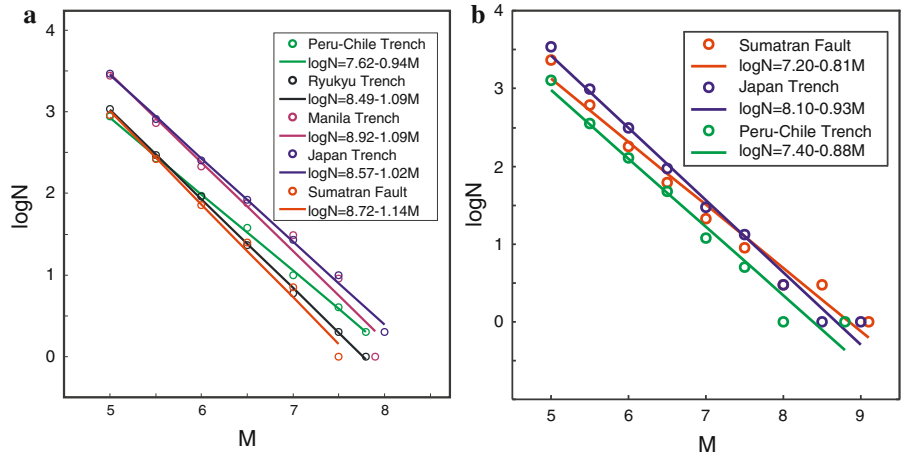

Figure 1

Fitted lines of G-R relationships in the trench regions. **a** *Fitted lines* respond to B cases. The time periods of seismic records are from 1 January 1973 to 25 December 2004 for the Sumatran fault, 26 February 2010 for the Peru-Chile trench, 10 March 2011 for the Japan trench, and 2 April 2011 for the Manila and Ryukyu trenches. **b** *Fitted lines* correspond to A cases. The time periods of seismic records are from 1 January 1973 to 2 April 2011

major earthquakes happened. Figure 1b shows the fitted lines of A cases. In Fig. 1b the time periods of the seismic records for the three regions are from 1 January 1973 to 2 April 2011.

According to the mathematical expressions of the G-R relationship, we calculated the return periods of earthquakes with magnitudes of 9.0 in these three trench regions. In the B cases, the return periods are around 151a for the Japan trench, 1075a for the Sumatran fault and 249a for the Peru–Chile trench. However, the actual major earthquakes happened in the 38th, 31st and 37th years in these three regions, respectively. In the A cases, the return periods are around 69a for the Japan trench, 46a for the Sumatran fault and 123a for the Peru-Chile trench. Therefore, using the seismic records before major earthquake events would underestimate the possibility, whereas using the records after that would overestimate the possibility of a mega-earthquake. It is possible to infer the conclusion that the possibility of major earthquakes cannot be predicted by the extrapolation of the G-R relationship. This is partly due to the short time windows of the earthquake records, which may need a very long period, ranging from several 100 to 1,000 years, to acquire more general conclusions. For the Manila and Ryukyu trenches, the return periods of earthquakes with magnitudes of 9.0 are 287a and 773a, which correspond to the B cases. It is therefore reasonable to make a prediction that the return periods of huge earthquakes may be shorter than what we got from the G-R relationship along these two trenches.

Furthermore, it's unnecessary for major earthquakes to essentially trigger tsunamis. Rather than computing the probabilities of the tsunamigenic earthquakes as in previous work (Liu *et al.*, 2007), we investigated the percentage of tsunami-associated earthquakes in the total number of earthquakes during the past approximately 100 years. We analyzed the seismic data for the time period from 1900 AD to 2011 AD, which were downloaded from The Significant Earthquake Database of the National Geophysical Data Center (NOAA http://www.ngdc.noaa.gov/nndc/struts/form?t=101650&s=1&d=1). We counted the earthquakes with magnitudes greater than or equal to *M* and found those associated with tsunamis. The statistical percentages are plotted in Fig. 2.

Figure 2 shows the percentages of tsunami-associated earthquakes during the past approximately 100 years. In general, the greater the magnitude is, the higher the percentage of the tsunamis associated with earthquakes. The low percentage of earthquakes of M8.0 or greater might be attributed to the lack of tsunami measurements during those events. Some of these earthquakes may have generated tsunamis that were not reported or measured, especially the older

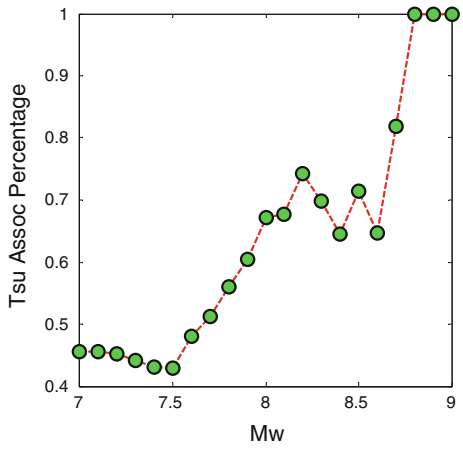

Figure 2
The statistical percentages of tsunami-associated earthquakes in the total number of earthquakes with magnitudes greater than or equal to M

events, because of the unavailability of tsunami detection technology. Especially earthquakes with magnitudes equal to or greater than 8.8 all triggered tsunamis; mega-earthquakes usually happen along the trench regions where they are overlaid by several kilometers of sea water. When these earthquakes happen, they provide a dislocation of the seafloor that allows a quick and efficient transferring of energy from the solid earth to the ocean, which causes tsunamis. So if M_w 8.8 or greater earthquakes occur in the Manila or Ryukyu trench, they are most likely to produce disastrous tsunamis.

According to the above-mentioned analyses, we proposed numerical simulations to evaluate the potential tsunami hazards caused by M_{w} 8.8 earthquakes along the Manila and Ryukyu trenches. The fault parameters were assigned according to the magnitude level and local geological background. Based on seismological theory, the important quantity in theoretical relationships between moment magnitude and fault parameters is seismic moment, $M_o = \mu \cdot \Delta U \cdot L \cdot W$, where μ is the shear modulus of the rocks involved in the earthquake, ΔU is the average displacement on the area of the rupture along the geologic fault where the earthquake occurred, L is the length along the strike, and W is the width along the dip. The relationship between the seismic moment and moment magnitude is $M_o = 10^{1.5M_w+9.1}$. Given that M_{w} is equal to 8.8, we can calculate the M_o as one confinement of the fault parameters. In addition, we noticed that mega-earthquakes usually happen in the continental plate side along the subduction zones where the dense oceanic plate descends beneath the lighter continental plate. We deployed potential tsunami sources located along these two trenches separately. Fault parameters were assigned according to the magnitude level and local geological situations mentioned above, which are listed in Table 2.

2.2. Numerical Modeling

Our numerical simulation models are based on shallow-water equations (SWE) as follows:

$$\begin{cases} \frac{\partial u}{\partial t} + g\frac{\partial \eta}{\partial x} = fv \\ \frac{\partial v}{\partial t} + g\frac{\partial \eta}{\partial y} = fu \\ \frac{\partial \eta}{\partial t} + \frac{\partial (Hu)}{\partial x} + \frac{\partial (Hv)}{\partial y} = 0 \end{cases} \quad \begin{array}{l} \eta(x,y,t); \\ \text{the vertical displacement} \\ \text{of free surface,} \\ \mathrm{H}(x,y); \text{the still water depth.} \end{array}$$

The finite difference method is a convenient way to solve the SWE numerically. This method is also employed by many well-known models, such as

Table 2
Fault parameters of the hypothetical tsunami sources in the Manila and Ryukyu trenches

Fault parameters	Epicenter	Strike angle	Dip angle	Slip angle	Length (km)	Width (km)	Average displacement (km)	Depth (km)
M_{w} 8.8 earthquake in Manila trench	16.5°N 119.0°E	180°	14°	81°	300	100	22.2	24
M_{w} 8.8 earthquake in Ryukyu trench	23.6°N 126.0°E	255°	14°	81°	300	100	22.2	24
M_{w} 8.0 earthquake in Ryukyu trench	23.6°N 126.0°E	255°	14°	81°	200	90	2.3	24

COMCOT (Liu *et al*., 1998), TUNAMI (Imamura and Shuto 1988) and MOST (Titov and Synolakis, 1997). The propagation of tsunami waves is modeled using TUNAMI N1 software. TUNAMI is the outcome of the UNESCO TIME Project and released by Fumihiko Imamura. Yalciner et al. simulated the 26 December 2004 Indian ocean tsunami and compared it with a field survey (Yalciner *et al*., 2005), which verified this code. A dozen boundary conditions have been proposed in the literature (Marchesiello *et al*., 2001; Palma and Matano, 2001). In our numerical models, the open boundary condition, which means free outward passage of the wave at the open sea boundaries, was employed. It approximates the practical situation (Agoshkov *et al*., 1994; Bresch, 2009).

In our model, we adopted the topographic and bathymetric data from the Shuttle Radar Topography Mission (SRTM) (Jarivs *et al*., 2008). During the construction of the computing domains, different precisions of topography SRTM30_plus data (30 arc second resolution data) include both the land and ocean area ftp://topex.ucsd.edu/pub/srtm30_plus/. The SRTM30_plus was developed from a wide variety of data sources including the NOAA, individual scientists, SIO, NGA, JAMSTEC IFREMER, GEBCO and NAVOCEANO (Becker *et al*., 2009), and SRTM3 data (3 arc second resolution data only in the land area http://srtm.csi.cgiar.org/) have been integrated in order to obtain higher resolution of the coastlines. Initial sources of tsunamis were generated in the form of an Okada elastic dislocation solution (Okada, 1985). We used (2001 × 2001) finite-difference grid points in the first level simulations, and the spatial grid resolution was around 3000 m. Multi-scale simulation with higher resolution was used to investigate the edge waves diffracted around Taiwan, while the grid size of the second level was around 380 m.

3. Numerical Simulation Results

The validity of the linear model has been discussed in previous work (Yalciner *et al*., 2004). We used commercial software (Amira GmbH., 2011) for the visualization (Zhang *et al*., 2008). By visualizing the results from the numerical simulation, we generated animations that illustrated the reflection, refraction, diffraction and interaction of the shallow-water waves. Snapshots of the animations are shown in Fig. 3, describing the characteristics of the tsunami waves' propagation.

Taking the tsunami generated by the M_w 8.8 earthquake in the Ryukyu trench as an example, Fig. 3 shows the characteristics of tsunami propagation. Since the water depth near the Chinese coast is much shallower than that of the Pacific Ocean, the speed of wave propagation becomes much slower. This can be observed from the wave crests, which were drawing near to each other. At the same time, the wave height increases to a devastating surge scale. In this case, even the wave height remains relatively small in the ocean; it becomes higher and leads to hazards when it arrives at the harbor area.

The distribution of maximum tsunamis directly revealed the dimension of the tsunami hazards. Figure 4 shows a map of the maximum free-surface tsunami elevation. Figure 4a is the maximum tsunami map of an M_w 8.8 earthquake occurring in the Manila trench. In this case, the most dangerous area is the South China Sea coast. Similarly, Fig. 4b is the maximum tsunami map of an M_w 8.8 earthquake occurring in the Ryukyu trench, while the most dangerous area is the East China Sea coast. Consequently, we also did a simulation of an M_w 8.0 earthquake occurring in the Ryukyu trench. Figure 4c shows the results of that case. Note that the color map of Fig. 4c ranges from 0 to 1 m, which means that the degree of danger in this situation is much lower than that of M_w 8.8 earthquakes. The maximum tsunami map indicates that the Shanghai and Hangzhou Bay areas are the most vulnerable regions. One interesting finding is that even though Taiwan is nearest to the source of the tsunami, the maximum tsunami is not observed in these cases. One of the major reasons could be that Taiwan lies right on the extension of the scenario fault strike line. However, the bathymetry of the sea bed near the eastern Taiwan coast varies sharply. This will induce serious surge waves. Moreover, the fault strike is precisely known, and the run-up process is still somewhat uncertain in our numerical model; in the future more attention should be paid to the potential tsunami hazard in Taiwan.

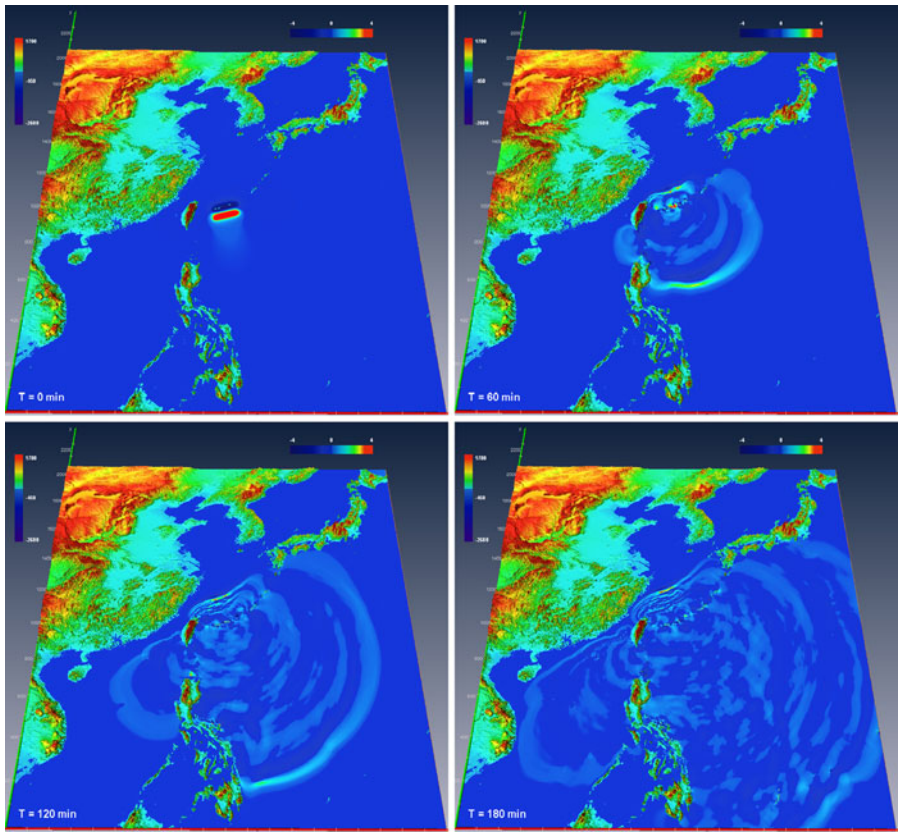

Figure 3
Tsunami simulation results taking the Ryukyu trench as scenario source. **a–d** Snapshots of $t = 0$ min, $t = 60$ min, $t = 120$ min and $t = 180$ min, respectively. The color map for tsunami wave height in the upper right corner of each *panel* ranges from −4 to 4 m

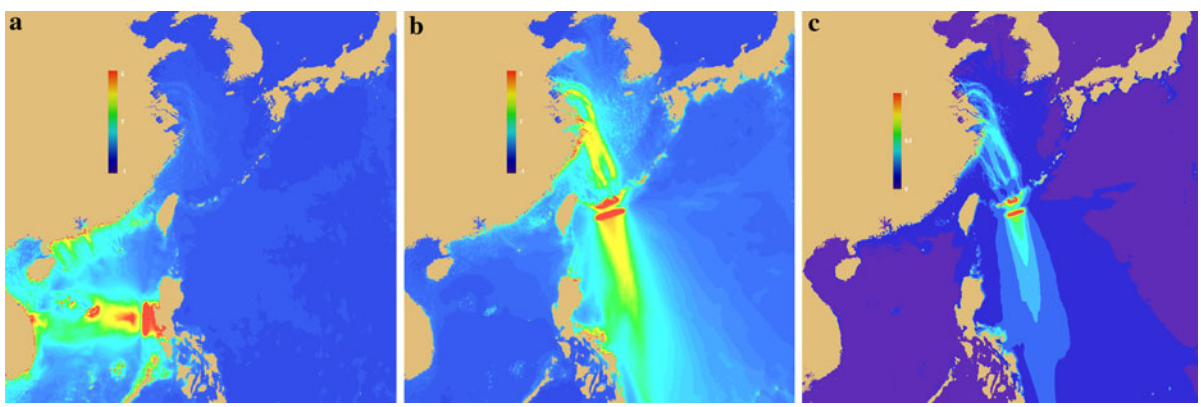

Figure 4
The peak tsunami height distribution maps in different cases. **a** The peak tsunami height distribution map from an M_w 8.8 earthquake occurring in the Manila trench. The color map range is from −1 to 5 m (case a). **b** The peak tsunami height distribution map from an M_w 8.8 earthquake occurring in the Ryukyu trench. The color map range is from −1 to 5 m (case b). **c** The peak tsunami height distribution map from an M_w 8.0 earthquake occurring in the Ryukyu trench. The color map range is from 0 to 1 m (case c)

Furthermore, we set some virtual tidal-wave gauges in the harbors along the Chinese coast. Table 3 lists the location of the gauges and the maximum wave height records at these points in different models. Cases a to c are in one-by-one correspondence to the models shown in Fig. 4. If the

Table 3

The location of the virtual wave gauges and the maximum tsunami wave height in different models

Wave gauges	Location Longitude, latitude	Case a	Case b	Case c
Dalian	38.8°N 121.7°E	0.0	0.1	0.0
Yantai	37.5°N 121.6°E	0.0	0.3	0.0
Tsingtao	35.9°N 120.4°E	0.1	0.6	0.1
Shanghai	31.2°N 121.3°E	0.5	6.2	0.7
Hangzhou Bay	30.5°N 122.6°E	0.1	2.5	0.2
Ningbo	30.0°N 122.5°E	0.6	4.7	0.5
Wenzhou	27.9°N 121.6°E	0.3	2.3	0.2
Fuzhou	26.1°N 120.2°E	0.6	1.2	0.1
Keelung	25.2°N 121.8°E	0.3	1.4	0.1
Hualien	24.0°N 121.6°E	0.5	2.9	0.4
Taitung	22.7°N 121.2°E	0.9	1.5	0.2
The southern tip of Taiwan Island	21.9°N 120.8°E	0.6	1.2	0.2
Pingtung	22.3°N 120.5°E	1.5	1.4	0.1
Tainan	22.9°N 120.1°E	1.7	1.4	0.2
Kaohsiung	22.6°N 120.2°E	1.8	1.8	0.2
Penghu Islands	23.6°N 119.6°E	1.5	0.8	0.1
Quanzhou	24.7°N 118.9°E	1.1	1.0	0.1
Xiamen	24.3°N 118.2°E	1.1	1.5	0.1
Shantou	23.3°N 116.9°E	2.5	1.3	0.1
Hong Kong	22.1°N 114.2°E	2.8	0.7	0.1
Macau	22.1°N 113.6°E	4.6	1.3	0.1
Zhanjiang	21.1°N 110.7°E	5.1	1.1	0.1
Haikou	20.1°N 110.2°E	0.8	0.2	0.1
Sanya	18.0°N 109.6°E	2.2	0.3	0.0

earthquake magnitude is equivalent to M_w 8.8, the highest tsunami wave from the Manila trench will be 5.1 m when it hits Zhenjiang and Guangdong provinces, while the highest tsunami wave reaches 6.2 m when it arrives in Shanghai if the same magnitude earthquake occurs along the Ryukyu trench. If the magnitude of the earthquake happening in the Ryukyu trench is 8.0, the highest wave in Shanghai is also 0.7 m. These phenomena force us to pay more attention to constructing an earthquake-reduced tsunami warning system in this region in the future.

4. Multi-Scale Simulation Results

We also carried out multi-scale simulation in order to investigate the wave hazard over a small region. Our major motivation was to obtain a high-resolution solution while maintaining a reasonable computing costs. We first computed the whole simulation domain with a relatively coarser grid size. Gradually, the grid size was decreased, and the computing domain was decreased as well. The boundary and initial values on the refined grids were interpolated from that of the larger domain size directly. By repeating these data transfer and computing processes, we eventually got a "focus" effect on the target coastal area, such as the Taiwan region, which is shown in Fig. 5. Using this methodology, we can utilize the highest resolution coastline and bathymetric data at the same time. Furthermore, this method can be facilitated on a massively parallel cluster, which can greatly reduce the computing time.

Obviously, there is wave diffraction around Taiwan Island. These results provide us with much detailed information on the region we are interested in, such as some cities with large populations and developed areas, and economic or political centers. The diffractions around Taiwan and their difference between the southern and northern parts of Taiwan Island are clearly shown in Fig. 5. The water depth on the eastern side of Taiwan is much deeper than that on the northeastern side, which induced different refractions. These phenomena can be found according to the distance of the wave crest, which is larger in the south than in the northeast. Since there is low bottom friction in the deep ocean of east Taiwan, the tsunamis with long wave length diffracted around the southern tip of Taiwan still bring in tremendous kinetic energy and will cause a very high surge along the coastal area.

5. Discussions and Conclusions

The potential tsunami hazards from the Manila and Ryukyu trenches to the South China and East China Seas were highlighted by Japan's 2011 Tohoku earthquake and the attendant tsunami. By using the historical seismic records from the NEIC in the approximately last 4 decades, we calculated the return periods in two cases and concluded that using the seismic records before the major earthquake events would underestimate the possibility, while using the records after that would overestimate the possibility of mega-earthquakes. We argue that major earthquakes in the Manila and Ryukyu trenches are more of a risk than than extrapolated by the local G-R

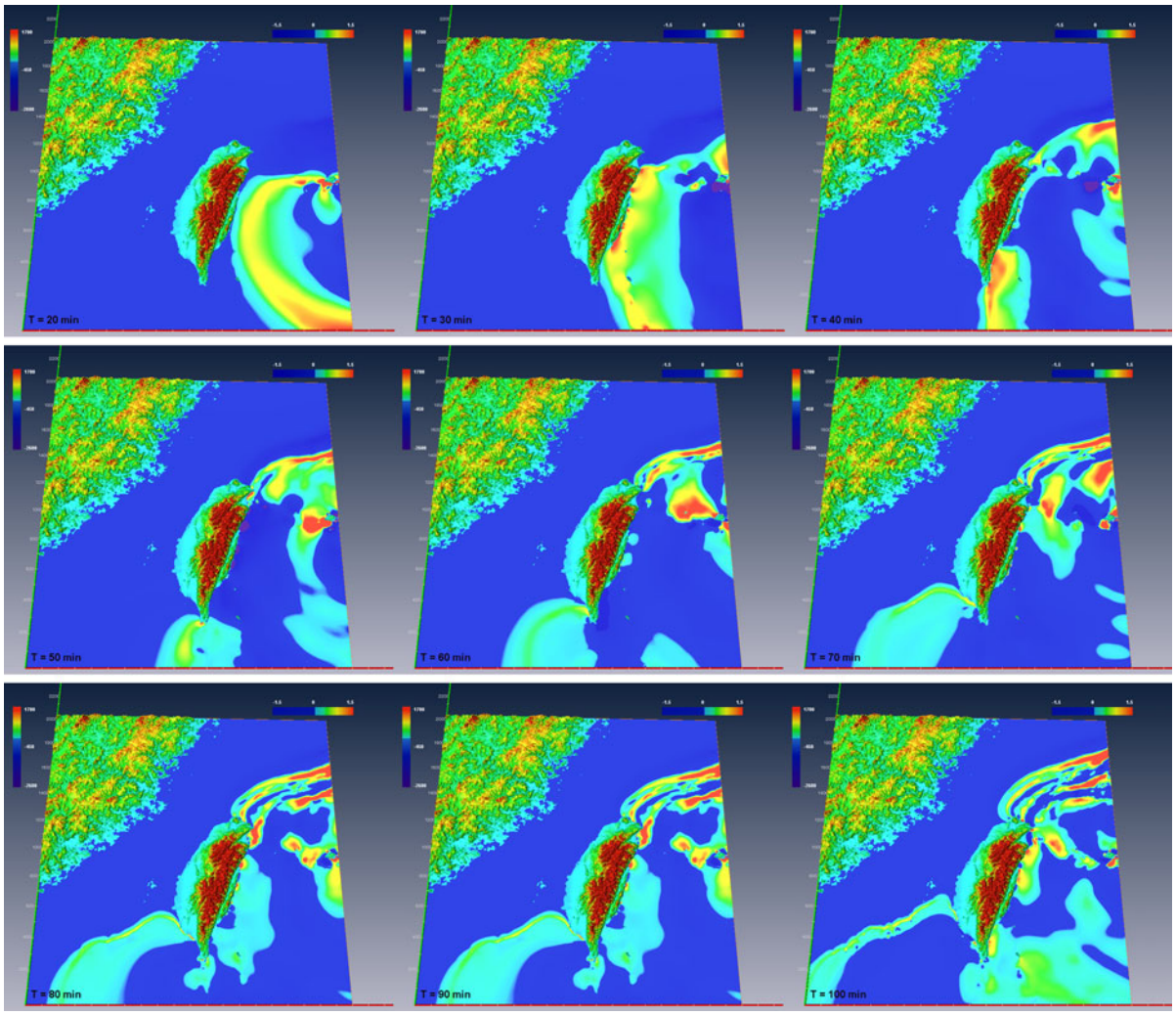

Figure 5
Multi-scale simulation results focusing on diffracted waves, taking the sub-domain around Taiwan as the initial values and boundary condition. The time steps are shown in the lower left corner of every snapshot, which are from the 20th to 100th min, with an interval of 10 min

relationship with the current several decades' seismic records. Furthermore, we investigated the percentage of tsunami-associated earthquakes in the total number of earthquakes during the past approximately 100 years. We emphasized here that the greater the magnitude is, the higher the percentage of tsunamis associated with the earthquakes. If earthquakes with magnitudes equal to or greater than M_w 8.8 occur along the Manila or Ryukyu trench, they are most likely to produce very disastrous tsunamis.

We proposed numerical simulations based on a shallow-water equation to evaluate the wave hazards along the southern and eastern Chinese coasts in order to investigate the effects of different tsunamis from these two trenches. Our primary results from the different cases show that tsunamis generated by M_w 8.8 earthquakes in the Manila trench will produce a significant threat to Guangdong province. The highest tsunami will be 5.1 m and will occur at Zhenjiang. A major earthquake in the Ryukyu trench would generate dangerous tsunamis in the East China Sea. The highest tsunami will be more than 6 m and will occur near Shanghai. The tsunami in Taiwan is not the highest, which is somewhat surprising. This is

partially because it lies right on the extension of the fault strike line scenario. In our current models, the local high-resolution topography and bathymetric data along the eastern Taiwan coastline are not included, and the run-up inundation has not been addressed in high-resolution simulations. Although the current tsunami wave pattern height looked almost the same as in other regions, the tsunami wavelengths were not actually the same. Especially the topography of the sea bed near the coast of eastern Taiwan has rather sharp features, which will greatly enhance the tsunami wave during the run-up process. Since the exact fault strike is unpredictable and the run-up process is still lacking in our numerical model, the potential tsunami hazard in Taiwan should be given more attention in future studies, especially in the Keelung and Penghu Island regions.

Our current work provided the preliminary estimation of tsunamis in the South China and East China Seas. We are planning to make more calculations of earthquakes at different locations and with varied magnitudes. By statistical analysis, we can obtain a complete and detailed hazard map of Chinese coastline regions. Furthermore, harbors have different shapes, bathymetric profiles, and other hydrological and geological characteristics, and their own Eigen periods of standing waves are different. The standing waves would induce oscillations in harbors of variable depth (WANG *et al.*, 2011; MATTIOLI, 1978). By adopting multi-scale numerical methodology and power spectrum density analysis tools, we can obtain the Eigen-period map of the respective harbor and propose appropriate tactics for improving harbor defense in the future.

Acknowledgments

The work was supported by the Chinese Deep Crust Exploration Project Sino-Probe 07, National High Technology Research and Development Program of China (863 Program) (no. 2010AA012402) and the K.C. Wong Magna Fund of Ningbo University. Dave Yuen thanks the CMG program of the US National Science Foundation. This research received technical assistance from the Minnesota Supercomputing Institute.

REFERENCES

JARVIS, A., REUTER, H. I., *et al.* (2008). Hole-filled seamless SRTM data V4, International Centre for Tropical Agriculture (CIAT), available from http://srtm.csi.cgiar.org.

AGOSHKOV, V. I., QUARTERONI, A., *et al.* (1994). "*Recent developments in the numerical simulation of shallow water equations I: boundary conditions*." Applied Numerical Mathematics *15*(2): 175-200, doi:10.1016/0168-9274(94)00014-x.

BRESCH, D. (2009). Shallow-Water Equations and Related Topics. Handbook of Differential Equations: Evolutionary Equations. Dafermos and Pokorny, North-Holland. Volume *5*: 1-104.

CATHERINE, J. K., GAHALAUT, V. K., *et al.* (2005). "*Constraints on rupture of the December 26, 2004, Sumatra earthquake from far-field GPS observations*." Earth and Planetary Science Letters *237*(3-4): 673-679, doi:10.1016/j.epsl.2005.07.012.

FUKAO, Y. (1979). "*Tsunami Earthquakes and Subduction Processes Near Deep-sea Trenches*." Journal of Geophysical Research *84*(NB5): 2303-2314.

GAHALAUT, V. K., NAGARAJAN, B., *et al.* (2006). "*Constraints on 2004 Sumatra-Andaman earthquake rupture from GPS measurements in Andaman-Nicobar Islands*." Earth and Planetary Science Letters *242*(3-4): 365-374, doi:10.1016/j.epsl.2005.11.051.

GELLER, R. J. (2011). "*Shake-up time for Japanese seismology*." Nature *472*(7344): 407-409, Amira. from http://www.amiravis.com/.

GUTENBERG, B. and RICHTER, C. F. (1944). "Frequency of earthquakes in California." BULLETIN OF THE SEISMOLOGICAL SOCIETY OF AMERICA *34*(4): 185-188.

HAYES, D. E. and LEWIS, S. D. (1985) "*Structure and tectonics of the Manila trench system, Western Luzon, Philippines*." Energy *10*(3-4): 263-279, doi:10.1016/0360-5442(85)90046-5.

IMAMURA, F., SHUTO, N., and GOTO, C., (1988). Numerical simulations of the transoceanic propagation of tsunamis. 6th Congress APD-IAHR, Kyoto, Japan.

J. J. BECKER, D. T. SANDWELL, W. H. F. SMITH, J. BRAUD, B. BINDER, J. DEPNER, D. FABRE, J. FACTOR, S. INGALLS, S-H. KIM, R. LADNER, K. MARKS, S. NELSON, A. PHARAOH, R. TRIMMER, J. VON ROSENBERG, G. WALLACE, P. WEATHERALL, (2009). *Global Bathymetry and Elevation Data at 30 Arc Seconds Resolution: SRTM30_PLUS*. Marine Geodesy, *32* (4).

KU, C.-Y. and HSU, S.-K. (2009). "*Crustal structure and deformation at the northern Manila Trench between Taiwan and Luzon islands*." Tectonophysics *466*(3-4): 229-240, doi: 10.1016/j.tecto.2007.11.012.

LIU, N., NIU, F., *et al.* (2010). "*Imaging the rupture of the 2010 M8.8 Chile earthquake with a broadband seismic array*." China Journal of geophusics *53*(7): 1605-1610.

LIU, P. L.-F., WOO, S. B., *et al.* (1998). Computer Programs for Tsunami Propagation and Inundation. Cornell University, Sponsored by National Science Foundation: 104.

LIU, P. L. F., WANG, X., *et al.* (2009). "*Tsunami hazard and early warning system in South China Sea*." Journal of Asian Earth Sciences *36*(1): 2-12, doi:10.1016/j.jseaes.2008.12.010.

LIU, Y., SANTOS, A., *et al.* (2007). "*Tsunami hazards along Chinese coast from potential earthquakes in South China Sea*." Physics of The Earth and Planetary Interiors *163*(1-4): 233-244.

MARCHESIELLO, P., MCWILLIAMS, J. C., *et al.* (2001). "*Open boundary conditions for long-term integration of regional oceanic models*." Ocean Modelling *3*(1-2): 1-20.

Mattioli, F. (1978). "*Wave-induced oscillations in harbours of variable depth*." Computers & Fluids *6*(3): 161-172, doi: 10.1016/0045-7930(78)90023-3.

Megawati, K., Shaw, F., *et al.* (2009). "*Tsunami hazard from the subduction megathrust of the South China Sea: Part I. Source characterization and the resulting tsunami*." Journal of Asian Earth Sciences *36*(1): 13-20, doi:10.1016/j.jseaes.2008.11.012.

Okada, Y. (1985). "*Surface deformation due to shear and tensile faults in a half-space*." Bulletin of the Seismological Society of America *75*(4): 1135-1154.

Ozawa, A., Tagami, T., *et al.* (2004). "*Initiation and propagation of subduction along the Philippine Trench: evidence from the temporal and spatial distribution of volcanoes*." Journal of Asian Earth Sciences *23*(1): 105-111, doi:10.1016/s1367-9120(03)00112-3.

Palma, E. D. and Matano, R. P. (2001). "*Dynamical impacts associated with radiation boundary conditions*." Journal of Sea Research *46*(2): 117-132,.

Rangin, C., Stephan, J. F., *et al.* (1988). "*Seabeam survey at the southern end of the Manila trench. Transition between subduction and collision processes, offshore Mindoro Island, Philippines*." Tectonophysics *146*(1-4): 261-278, doi:10.1016/0040-1951(88)90095-9.

Sipkin, S. A., Person, W. J., *et al.* (2000). Earthquake Bulletins and Catalogs at the USGS National Earthquake Information Center, available from: http://earthquake.usgs.gov/earthquakes/eqarchives/epic/, U.S. Geological Survey National Earthquake Information Center.

Stein, S., Geller, R. J., *et al.* (2011). "*Bad assumptions or bad luck: why earthquake hazard maps need objective testing*." Seis. Res. Lett. *82*: 623-626.

Stein, S. and Okal, E. A. (2011). "*The size of the 2011 Tohoku earthquake need not have been a surprise*." EOS, TRANSACTIONS AMERICAN GEOPHYSICAL UNION *92*(27): 227.

Titov, V. V. and Synolakis, C. E. (1997). "*Extreme inundation flows during the Hokkaido-Nansei-Oki tsunami*." Geophysical Research Letters *24*(11): 1315-1318.

Turcotte, D. L., Shcherbakov, R., *et al.* (2007). Complexity and Earthquakes. Treatise on Geophysics. S. Gerald. Amsterdam, Elsevier: 675-700.

Wang, G., Dong, G., *et al.* (2011). "*An analytic investigation of oscillations within a harbor of constant slope*." Ocean Engineering *38*(2-3): 479-486, doi:10.1016/j.oceaneng.2010.11.021.

Yalciner, A., Pelinovsky, E., *et al.* (2004). "*Tsunamis in the Black Sea: Comparison of the historical, instrumental, and numerical data*." Journal of Geophysical Research-Oceans 109(C12) C1202310.1029/2003jc002113.

Yalciner, A. C., Perincek, D., *et al.* (2005) "December 26, 2004 Indian Ocean Tsunami Field Survey (Jan. 21-31, 2005) at North of Sumatra Island."

Zhang, H., L, S. Y., *et al.* (2008). "*Modeling and visualization of tsunamis*." Pure and Applied Geophysics *165*(3-4): 475-496. doi: 10.1007/s00024-008-0324-x.

(Received April 26, 2011, revised January 31, 2012, accepted March 2, 2012, Published online April 20, 2012)